

ANALYSIS OF THE VARIABILITY IN LAND SURFACE TEMPERATURE DUE TO LAND USE/LAND COVER CHANGE FOR A SUSTAINABLE URBAN PLANNING

ANUPAM PANDEY¹, ARUN MONDAL¹, SUBHANIL GUHA^{2*}, DURGESH SINGH¹,
RASHMI¹, SANANDA KUNDU³

¹*Department of Geography, University of Allahabad, Prayagraj, India*

²*Department of Applied Geology, National Institute of Technology Raipur, Raipur, India*

³*Department of Geography, Manipur University, Imphal, India*

*Corresponding author email: subhanilguha@gmail.com

Received: 10th September 2023, **Accepted:** 8th October 2023

ABSTRACT

In modern days, a sustainable urban planning system requires a balance of vegetation, water, and settlement. The proportions of these surface features directly influence the land surface temperature (LST) in an urban area. LST primarily depends on the emittance of land use/land cover (LULC) categories. In an urban area, changes in LULC categories as well as local warming are the prime regulators of LST change. The study analyses the LULC change and its impact on LST in Imphal City, India. Landsat satellite data for the summer season and winter seasons for 1991, 2001, 2011, and 2021 have been used in this study. Results show that the mean LST of the study area increased at >1% rate/decade. The green area and water area decreased the LST values whereas the built-up area and fallow lands increased the LST values. The study indicates the consequences of proper land conversion to regulate the LST change. Moreover, the influence of population on LST is also determined. The continuous rising trend of population is a positive factor of increasing LST. The study may help the town and country planners to generate sustainable urban land.

Keywords: Land surface temperature; Land use/land cover, Sustainable urban planning.

INTRODUCTION

Urbanization and land surface temperature (LST) can be considered a cause-and-effect relationship. Urban expansion leads to a rise in LST in almost all global cities. The rapid change in land surface material is a trademark signature of urban agglomerated landscape (Mushore *et al.*, 2021; Guha *et al.*, 2022). Influence of climate change also modifies the environmental status in a significant ratio (Kundu *et al.*, 2015, 2018; Mondal *et al.*, 2015, 2016a, 2016b, 2018). In an urban area, the land is mainly converted from the natural surface (vegetation, water, bare soil, or rock) into an artificial surface (road, building, factory, airport, car parking places, etc.) (Wiesner *et al.*, 2018; Karakuş, 2019). This type of land conversion accelerates the LST in mixed urban land and develops urban heat islands inside an urban body (Zhao *et al.*, 2016; Zhou *et al.*, 2019). Moreover, different categories of built-up surfaces generate different amounts of LST (e.g., a metalled surface can generate higher LST than an unmetalled surface like brick or glass material) (Balew & Korme, 2020).

Thus, analysis of land surface materials and their changes may be considered a crucial factor for LST rise in urban land (Peng *et al.*, 2016; Tran *et al.*, 2017; Guha & Govil, 2021).

Nowadays, many statistical algorithms describe the relation between LST and land surface indexes. For example, Feyisa *et al.* (2016) showed the impact of urban expansion and land cover mapping on the thermal condition of Addis Ababa city. Deilami & Kamruzzaman (2017) reviewed the impact of Land surface materials as a controlling factor of LST.

Derdouri *et al.* (2021) reviewed the interaction between land surface materials and the intensity of LST over two decades in urban landscapes. Dutta *et al.* (2020) tried to find the effect of land use change on urban heat islands for a long period in an industrial city in eastern India. Hashim *et al.* (2020) analysed the LST trend in Baghdad city and stated that the area of high LST has low vegetation coverage and vice versa. Alexander (2020) showed that the spectral indices formed by infrared bands generate better correlations with LST than the conventional NDVI or other vegetation indexes. Ayanlade (2016) investigated the seasonal impact of daytime and night-time LST on different land surface materials.

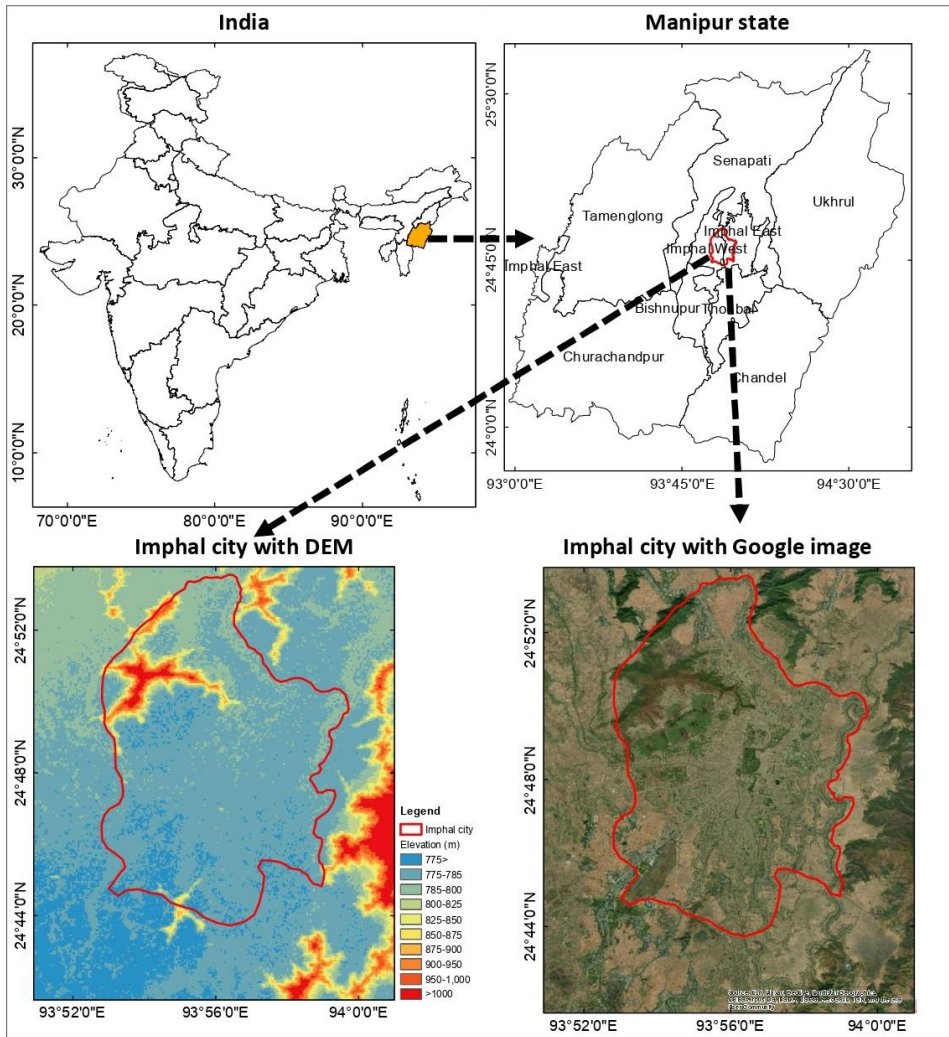
For sustainable town and country planning, the LST-LULC relationship is required as the various LULC types can directly influence the variation of LST. Hence, this LULC-based study is important in determining the stability of LST on any urban land surface (Guha & Govil, 2022). However, this type of analysis is rarely found in northeast India. Kalota (2016) and Mondal *et al.* (2021) investigated the characteristics of the surface temperature of Manipur State and Imphal City, respectively. Among the recent significant studies, Pandey *et al.* (2022a, 2022b, 2023a, 2023b) analyzed the relationship of LST with land surface indices in Imphal City. On this context, the current study analyzes the spatial distribution of the components which are used in determining the LST and the decadal information of population of the city. The study also attempts to evaluate the seasonal impact of different LULC categories on LST.

MATERIAL AND METHODS

Study area

The study area (Imphal city) extends from 24°53'47"N to 24°41'43"N and from 93°51'00"E to 94°01'00"E (Figure 1) and covers 420 km² surface area (Mondal *et al.*, 2021). The average elevation of the undulating surface of the city is approximately 800 m. The northwest portion reflects the higher relief whereas the southern part is characterised by the lower relief. The city is under a humid subtropical climate with warm humid summer and cool dry winter (<https://mausam.imd.gov.in/>). The maximum and minimum temperature of summer and winter is 30°C and 5°C, respectively. The mean temperature and the mean annual rainfall of the city are 20°C and 1450 mm, respectively. The nature of the soil is acidic alluvial and the vegetation types are moist evergreen and temperate (Mondal *et al.*, 2021). With many beautiful spots like Keibul Lamjao National Park, Imphal is considered a notable tourist place in northeast India (<https://imc.mn.gov.in/>). According to the 2011 census, the city has 0.27 million population (<https://censusindia.gov.in/>).

Fig. 1: Imphal city and adjacent area in SRTM DEM and Google image



Data

Four summer and four winter Landsat satellite data were obtained from the Earth Explorer website (<http://earthexplorer.usgs.gov/>) (Table 1). Shuttle Radar Topographic Mission Digital Elevation Model data was also downloaded for determining the surface elevation (<http://earthexplorer.usgs.gov/>). Here, this surface elevation map is shown for visualisation and understanding of the nature of LULC types. It is not used for determining LST or LULC types. The map and the necessary information about the city were taken from Imphal Municipal Corporation. Moreover, the Google Earth Image software was used to check the classified LULC map (<https://earth.google.com/web/>). ArcGIS and ERDAS Imagine software are used for various image-processing tasks. The data on weather conditions have also been provided here to compare the results (Table 2). The weather data for 2011 and 2021

are available but for 1991 and 2001 are not available (<https://mausam.imd.gov.in/>). As there are all cloud-free data, no record of precipitation is observed on these specific dates.

Table 1: Specification of the used Landsat satellite images

Landsat scene ID	Date of acquisition	Time (UTC)*	Path/Row	Sun elevation (°)	Sun azimuth (°)	Cloud cover (%)	Earth-Sun distance (astronomical unit)
Summer season							
LT51350431991108BKT00	18-Apr-91	03:34:00	135/043	56.09	108.42	7.00	1.00
LT51350432001135BKT01	15-May-01	03:52:12	135/043	64.13	97.29	5.00	1.01
LT51350432011099BKT01	09-Apr-11	04:01:51	135/043	59.68	119.96	0.00	1.00
LC81350432021110LGN00	20-Apr-21	04:11:42	135/043	64.64	116.66	9.64	1.00
Winter season							
LT51350431991028ISP00	28-Jan-91	03:32:37	135/043	34.42	137.09	1.00	0.98
LT51350432001039BKT00	08-Feb-01	03:52:05	135/043	39.76	138.59	0.00	0.99
LT51350432011035BKT00	04-Feb-11	04:02:01	135/043	40.21	142.28	0.00	0.99
LC81350432021014LGN00	14-Jan-21	04:12:14	135/043	37.97	149.60	7.94	0.98

*IST=UTC+05:30 (IST=Indian standard time, UTC=Coordinated universal time)

Table 2: Weather conditions for specific dates

Date	Air temperature (°C)	Wind velocity	Relative humidity	Precipitation (mm)	Weather condition
09-Apr-11	21.6	4km/h	34%	0	Scattered clouds
20-Apr-21	24.4	5km/h	78%	0	Fog
04-Feb-11	16.5	1km/h	61%	0	Sunny
14-Jan-21	15.1	3km/h	68%	0	Fog

Methods

The study computes the LST of eight satellite data. Moreover, the maximum likelihood supervised classification method with accuracy assessment is used to obtain the classified LULC maps. At the same time, the minimum, maximum, and mean values of annual AT and precipitation are also determined for the study period.

LST computation

LST computation sequentially follows some algorithms. These algorithms are as follows: At first, spectral radiance is calculated by Equation 1 (Artis & Carnahan, 1982):

$$L_{\lambda} = \text{RadianceMultiBand} \times DN + \text{RadianceAddBand} \quad (1)$$

L_{λ} = the spectral radiance in $\text{Wm}^{-2}\text{sr}^{-1}\text{mm}^{-1}$.

Thereafter, the at-sensor brightness temperature is calculated by Equation 2:

$$T_B = \frac{K_2}{\ln((K_1 / L_{\lambda}) + 1)} \quad (2)$$

Where, T_B = brightness temperature in Kelvin (K), L_λ = spectral radiance in $Wm^{-2}sr^{-1}mm^{-1}$; K_2 and K_1 = calibration constants.

Thereafter, fractional vegetation is calculated by Equation 3 (Carlson & Ripley, 1997):

$$F_v = \left(\frac{NDVI - NDV_{I_{min}}}{NDV_{I_{max}} - NDV_{I_{min}}} \right)^2 \quad (3)$$

Where, $NDV_{I_{min}}$ = minimum NDVI, $NDV_{I_{max}}$ = maximum NDVI. F_v = fractional vegetation.

Thereafter, land surface emissivity \mathcal{E} , is calculated by Equation 4 (Sobrino *et al.*, 2001, 2004):

$$\mathcal{E} = 0.004 * F_v + 0.986 \quad (4)$$

Where, \mathcal{E} = surface emissivity.

Finally, LST is calculated by Equation 5 (Weng *et al.*, 2004):

$$LST = \frac{T_B}{1 + (\lambda \sigma T_B / (hc)) \ln \mathcal{E}} \quad (5)$$

Where, λ = effective wavelength, σ = Boltzmann constant (1.38×10^{-23} J/K), h = Plank's constant (6.626×10^{-34} Js), c = velocity of light in a vacuum (2.998×10^8 m/sec), \mathcal{E} = emissivity.

Supervised classification

Landsat data from four years have been classified by applying the maximum likelihood supervised classification method. 120 sample points are used in this classification process. The final classes are water, forest, settlement, agriculture, and fallow land.

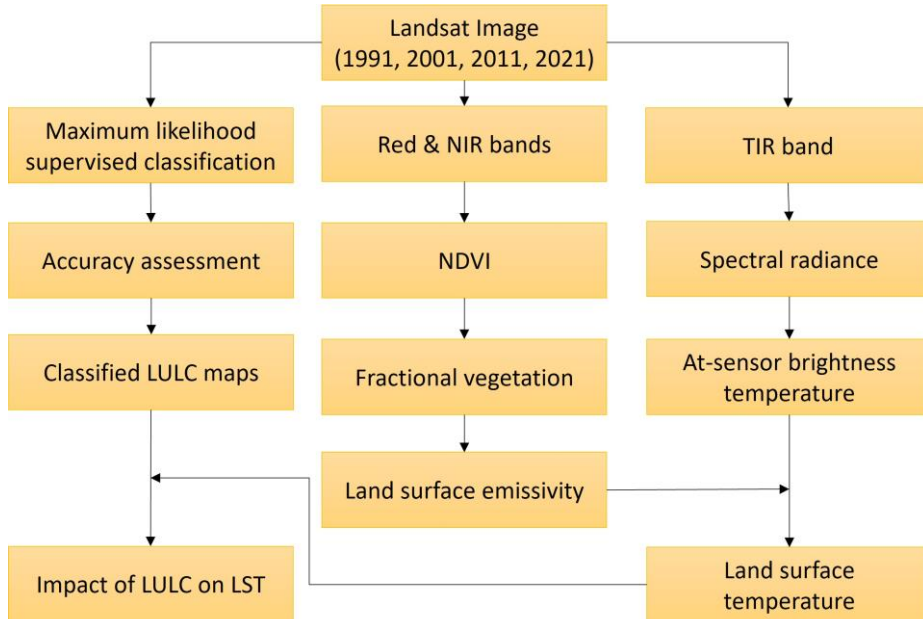
After that, overall accuracy and the Kappa coefficient techniques are used to determine the accuracy of the classification. The overall accuracy is determined by Equation 6:

$$\text{Overall accuracy} = \frac{\text{Number of correctly classified sample classes}}{\text{Number of reference sampling classes}} \quad (6)$$

The kappa coefficient is determined by Equation 7:

$$K = \frac{\text{Observed accuracy} - \text{Chance assessment}}{1 - \text{Chance agreement}} \quad (7)$$

Figure 2 represents the whole methodology of the study through a flow diagram.

Fig. 2: Methodology of the study

RESULTS AND DISCUSSION

Accuracy assessment of LULC classification

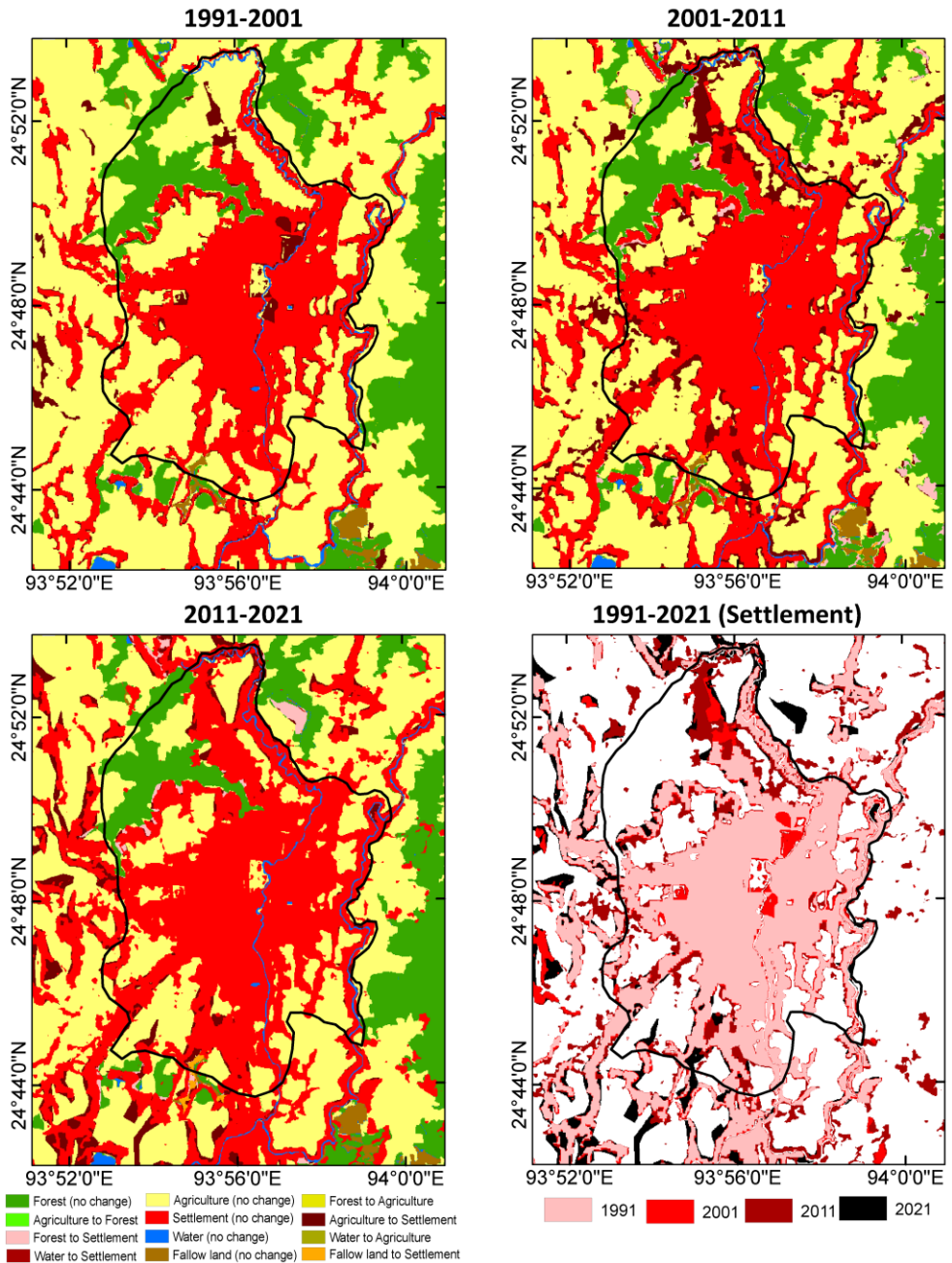
Table 3 represents the overall accuracy and Kappa coefficient values of five LULC classes. The overall accuracy values are 92 %, 92 %, 88 %, and 86 % in 1991, 2001, 2011, and 2021, respectively. Kappa coefficient values are 0.88, 0.88, 0.83, and 0.79 in 1991, 2001, 2011, and 2021. These results show that the classified LULC maps are almost accurate.

Table 3: Overall accuracy and Kappa coefficient values

Type	1991	2001	2011	2021
Overall accuracy	92%	92%	88%	86%
Kappa	0.88	0.88	0.83	0.79

Changing scenario of LULC types

Fig. 3: Changing scenarios in various LULC categories



Decadal changes in LULC types are shown in Figure 3. In this figure, five no-change classes (original classes found in supervised classification) have been presented. Besides, seven changed classes (forest-agriculture, water-agriculture, agriculture-forest, forest-settlement, water-settlement, fallow land-settlement, and agriculture-settlement) have also been presented. The highest number of changed pixels is observed in the settlement. Thus, a separate map of the changed settlement class has been shown in this figure (right bottom). Forest and agricultural land classes have been changed most (in terms of area) into settlement classes.

Changing scenario of NDVI, fractional vegetation (FV), and emissivity in the city

Fig. 4: Spatial distribution of NDVI (1991, 2001, 2011, 2021).

[Upper Part (A) - Summer, Lower Part (B) - Winter]

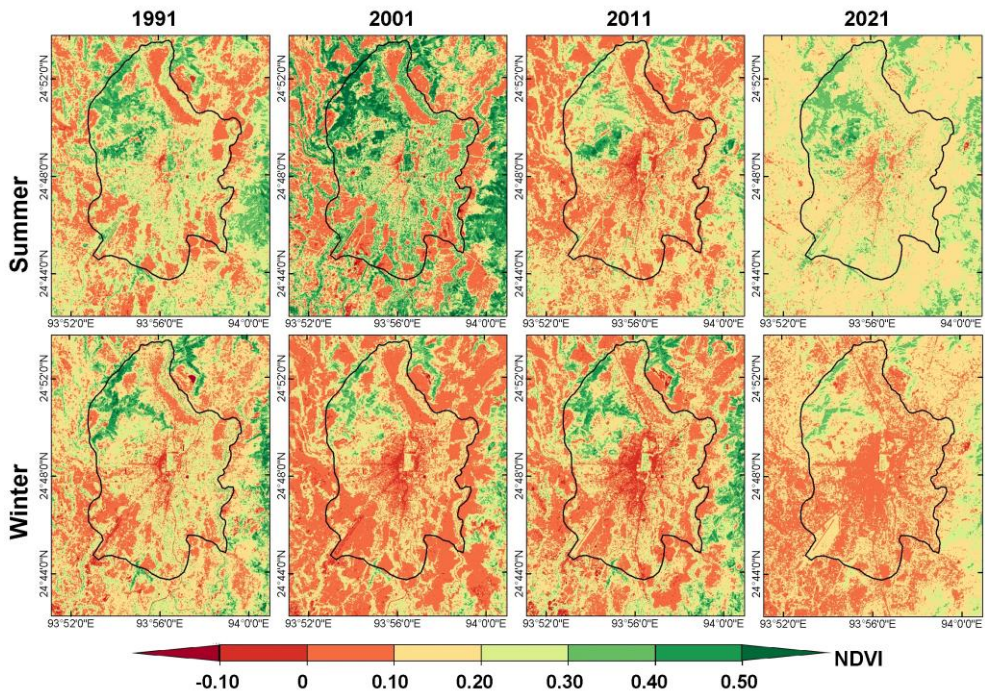


Figure 4 represents the spatial distribution of NDVI in the last 30 years. The green and water surface is decreased due to the expansion of built-up surface. The value and distribution of NDVI has been changed according to this type of change in surface area. The higher NDVI value (< 0.3) is found along the northern and eastern parts of the area. The summer season has more NDVI value than the winter season. LST than winter.

Fig. 5: Spatial distribution of FV (1991, 2001, 2011, 2021).

[Upper Part - Summer, Lower Part - Winter]

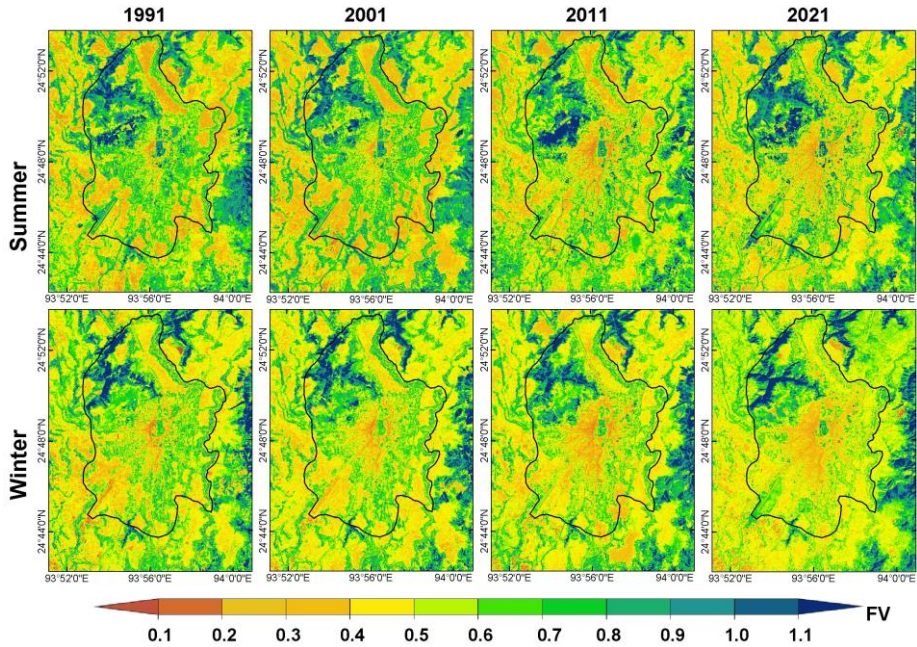


Fig. 6: Spatial distribution of emissivity (1991, 2001, 2011, 2021).

[Upper Part - Summer, Lower Part - Winter]

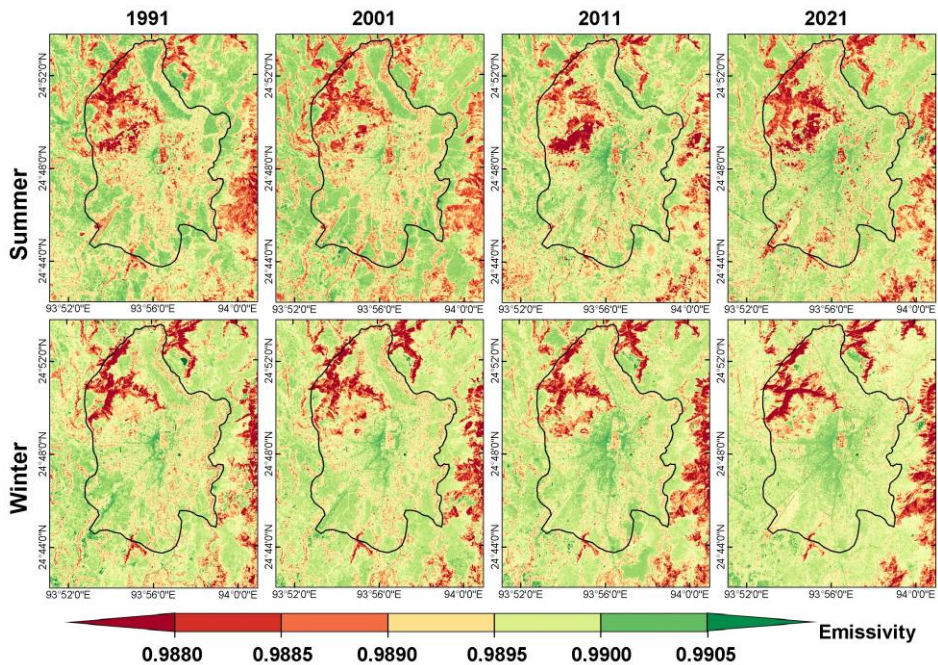


Figure 5 represents the spatial distribution of FV in the last 30 years. The higher concentration of vegetation reflects the higher values of FV (> 0.6). This scenario is observed in the northern and eastern portions of the study area. The summer and winter seasons show almost same value of FV.

Figure 6 shows the spatial distribution of emissivity during the period. Emissivity depends on the surface materials. Some built-up surface reflects higher emissivity that are visible in the central parts of the area. The summer and winter images have different status of emissivity. LST of any area directly proportionate to the values of emissivity.

Changing LST scenario in the city

Figure 7 represents the spatial LST distribution in the last 30 years. The total area under the green area and the water surface is reduced whereas the built-up surface areas are increased. The LST has been changed according to this land use change. The central and the northeast segments of the city gain more LST with time. The summer season witnesses more LST than winter. The middle part of the city became hotter after 2001. Both summer and winter season depicts the same picture.

Fig. 7: Spatial distribution (A) and decadal changes (B) of LST in summer.

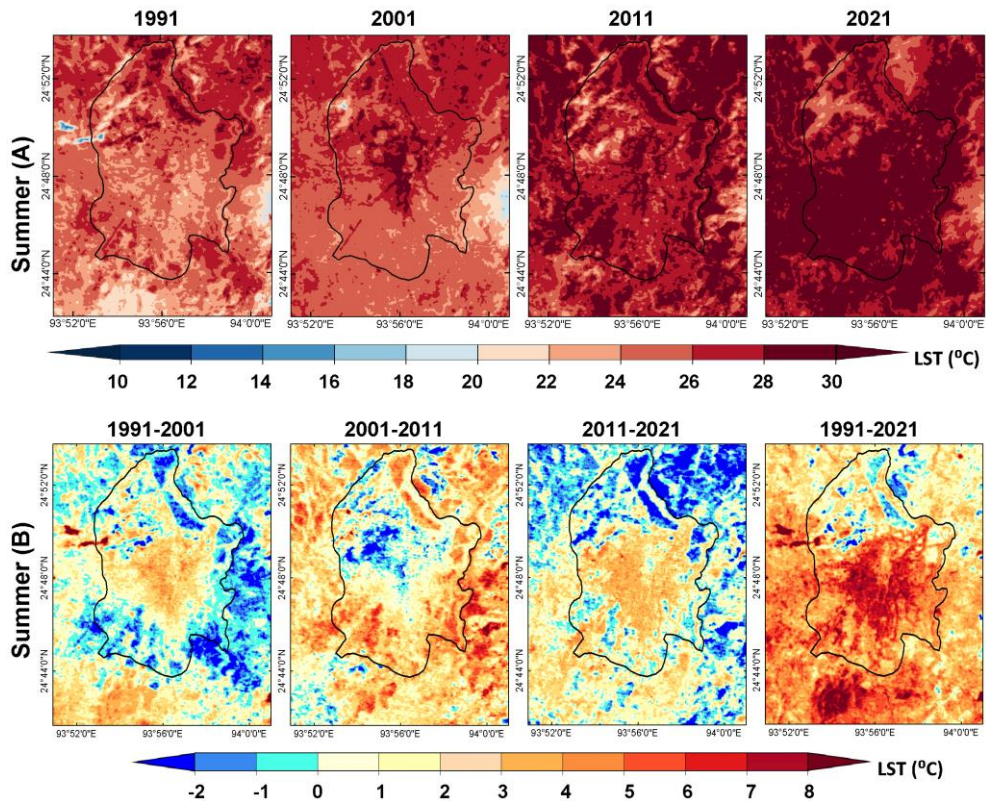


Figure 8 shows the decadal changes in LST difference in Imphal. LST increased a little bit in the central part between 1991 and 2001. However, during 2001-2011, the outer part experienced more LST. During 2011-2021, the central parts became warmer than the early

phases. From 2011-2021, the southern and central portions are substantially heated. This continuous warming is the consequence of fast land conversion in the area.

The decadal changes of LST (%) have been shown in Table 4. The highest increase (63 % and 42 % in summer and winter, respectively) has been noticed in the minimum LST values. Land conversion is the main factor for this decadal change in LST. During the entire summer season, LST rises 8°C, 6°C, and 3.5°C (approximately) on the minimum, maximum, and mean LST values. In the entire winter season, LST rises 3.5°C, 3°C, and 3°C (approximately) on the minimum, maximum, and mean LST values.

Fig. 8: Spatial distribution (A) and decadal changes (B) of LST in winter

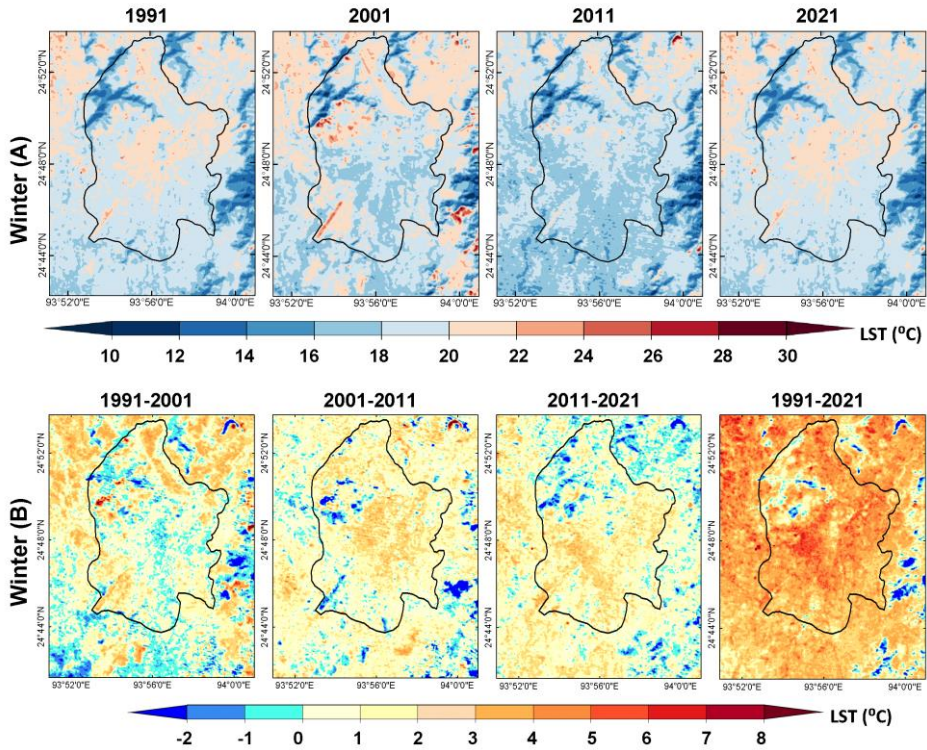


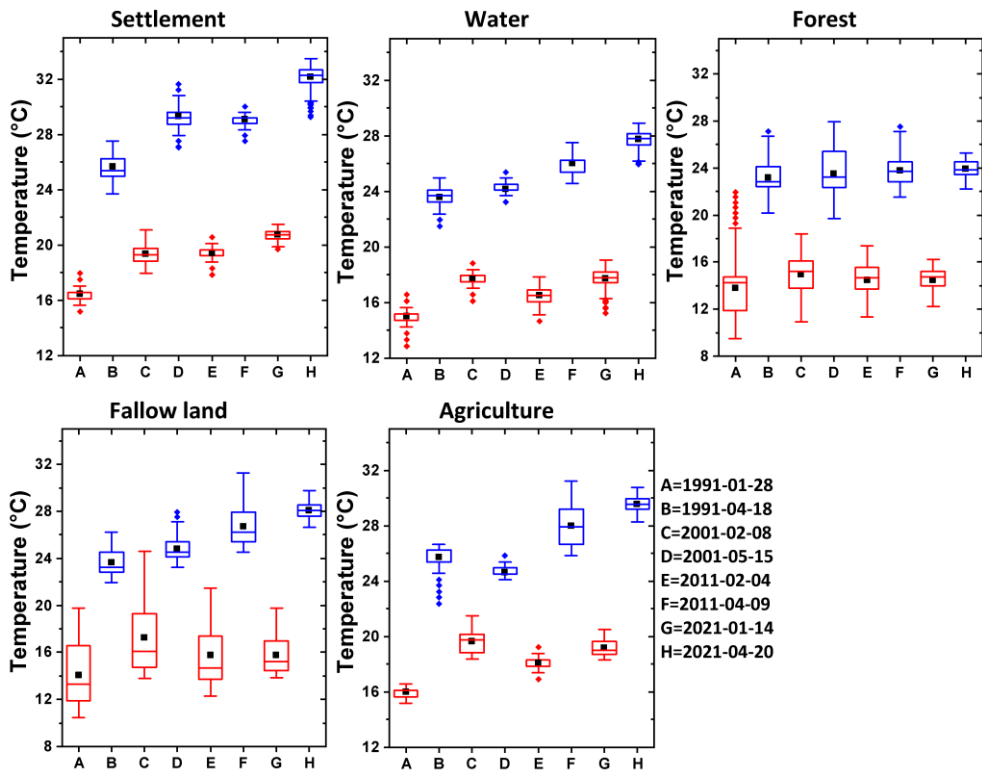
Table 4: Decadal changes (in %) of LST (°C)

Summer			
Year	LST(Min)	LST(Max)	LST(Mean)
1991-2001	27.81	-1.29	3.19
2001-2011	21.15	10.02	8.52
2011-2021	5.04	-1.44	2.16
1991-2021	62.73	7.02	14.39
Winter			
Year	LST(Min)	LST(Max)	LST(Mean)
1991-2001	24.47	8.91	21.15
2001-2011	-5.82	-11.04	-6.76
2011-2021	21.30	12.11	5.62
1991-2021	42.20	8.62	19.67

Impact of different LULC on LST generation

The minimum, maximum, median, upper quartile and lower quartile values of LST on separate LULC categories have been shown by box plot graphs (blue colour for summer and red colour for winter) in Figure 6. The highest and the lowest LST values (minimum, maximum, and mean) are observed on settlement and forest, respectively. The maximum range of LST is observed on fallow land and in the winter season. The median LST on fallow land is low in winter and high in summer. The median LST on settlement is high in summer and high to moderate in winter. The median LST in forest is low in summer and winter both seasons. The median LST on water bodies and agricultural land is moderate in summer and moderate to low in winter. The gradual increase of LST on every LULC type may be considered an indicator of constant local warming.

Fig. 9: Box plot graphs of LST on different LULC types



LST-population relationship during the study period

Figure 10 and 11 describe the relation of population with the summer LST and winter LST, respectively. Population of Imphal city rises abruptly from 1991 to 2021 (<https://www.ceicdata.com/en/india/census-population-by-towns-and-urban-agglomerations>). A lot of fluctuation is observed in the winter LST than summer LST. One of the interesting facts is that the trend of rising LST in the summer season is almost similar with the increasing trend of population. It clearly indicates that the significant rise of population increases a number of activities in domestic, commercial, industrial and transport sectors of the city those are directly responsible for the increase of LST in the city.

Fig. 10: LST-population relationship in summer

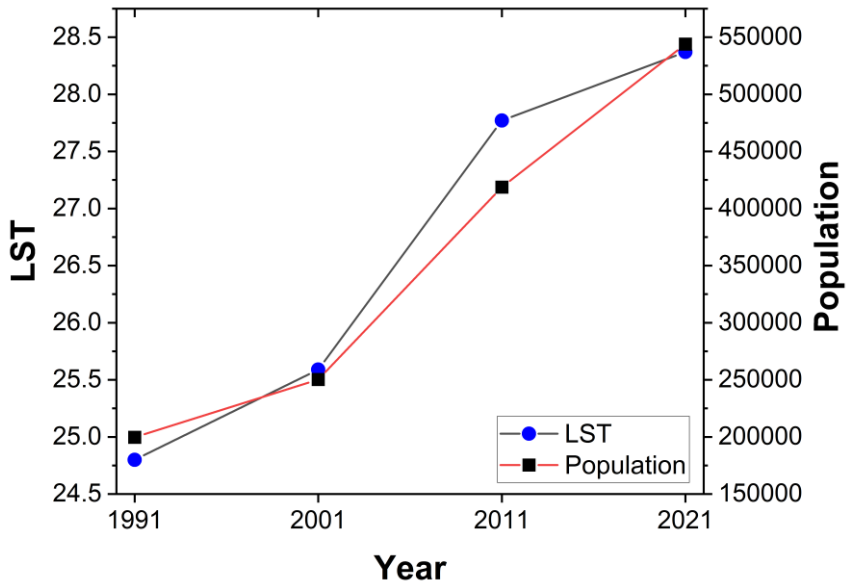
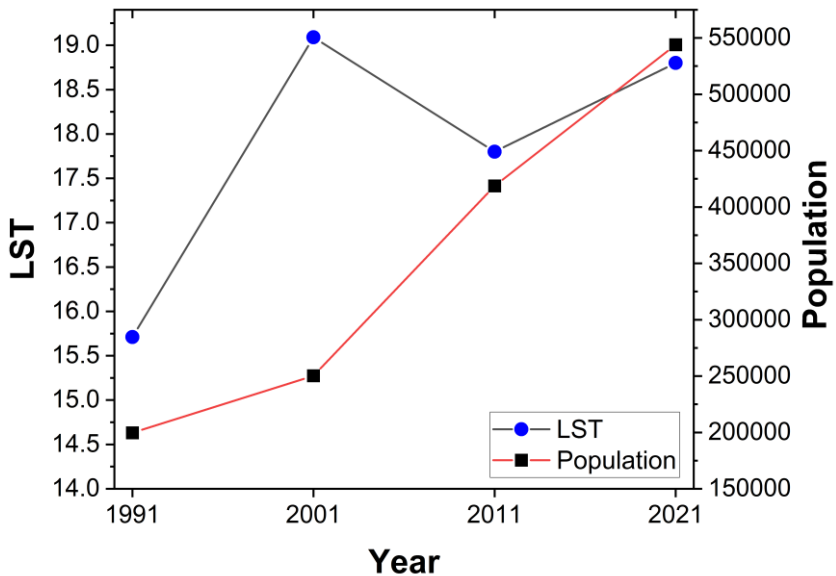


Fig. 11: LST-population relationship in winter



CONCLUSION

The present study determines the variation of LST and LULC for the last three decades in a northeast Indian city, Imphal. In summer and winter, LST increased at a rate of $>1^{\circ}\text{C}/\text{decade}$. Except for the northern part, LST rises significantly over the entire city. A constant rapid urban expansion has been seen in recent years in Imphal and it affects the LST of the city directly. The areas having a significant amount of green vegetation witness low LST and the areas other than green vegetation have high LST values. Land conversion may be considered the main factor for LST fluctuation. Mostly the vegetation surface has been converted into the fallow or barren land surface and LST varies significantly in those particular areas. Proper sustainable urban planning requires land conversion in a reverse way. The barren lands should be converted into agricultural land, grassland, or plantation cropland. It will check the LST status in the city. Moreover, the study also reflects the status of LST-population relationship in the city. The study is based on the summer and winter satellite data of four decades and other seasonal responses have not been recorded. It can be extended by investigating the satellites of other seasons maintaining a small interval of less than five years.

ACKNOWLEDGMENT

The authors are indebted to earth explorer website (<http://earthexplorer.usgs.gov/>).

COMPETING INTEREST

The authors declare no conflict of interest.

REFERENCES

- Alexander, C (2020). Normalised difference spectral indices and urban land cover as indicators of land surface temperature (LST). *Int J Appl Earth Obs Geoinf* 86: 102013. <https://doi.org/10.1016/j.jag.2019.102013>
- Artis, D.A., Carnahan, W.H. (1982). Survey of emissivity variability in thermography of urban areas. *Remote Sens Environ* 12(4), 313–329.
- Ayanlade, A. (2016). Seasonality in the daytime and night-time intensity of land surface temperature in a tropical city area. *Sci Total Environ* 557–558: 415–424. <https://doi.org/10.1016/j.scitotenv.2016.03.027>
- Balew, A., Korme, T. (2020). Monitoring land surface temperature in Bahir Dar city and its surrounding using Landsat images. *Egypt J Remote Sens Space Sci* 23(3): 371–386. <https://doi.org/10.1016/j.ejrs.2020.02.001>.
- Carlson, T.N., Ripley, D.A. (1997). On the Relation between NDVI, Fractional Vegetation Cover, and Leaf Area Index. *Remote Sens Environ* 62: 241–252. [https://doi.org/10.1016/S0034-4257\(97\)00104-1](https://doi.org/10.1016/S0034-4257(97)00104-1)
- Deilami, K., Kamruzzaman, M., Liu, Y. (2018). Urban heat island effect: A systematic review of spatio-temporal factors, data, methods, and mitigation measures. *Int J Appl Earth Obs Geoinf* 67: 30–42. <https://doi.org/10.1016/j.jag.2017.12.009>
- Derdouri, A., Wang, R., Murayama, Y., Osaragi, T. (2021). Understanding the Links

- between LULC Changes and SUHI in Cities: Insights from Two-Decadal Studies (2001–2020). *Remote Sens* 13(18): 3654. <https://doi.org/10.3390/rs13183654>
- Dutta, D., Gupta, S., Kishtawal, C.M. (2020). Linking LULC change with urban heat islands over 25 years: a case study of the urban-industrial city Durgapur, Eastern India. *J Spat Sci* 65(3): 501-518. <https://doi.org/10.1080/14498596.2018.1537198>
- Feyisa, G.L., Meilby, H., Jenerette, G.D., Pauliet, S. (2016). Locally optimized separability enhancement indices for urban land cover mapping: Exploring thermal environmental consequences of rapid urbanization in Addis Ababa, Ethiopia. *Remote Sens Environ* 175: 14-31. <https://doi.org/10.1016/j.rse.2015.12.026>
- Guha, S., Govil, H. (2021). A long-term monthly analytical study on the relationship of LST with normalized difference spectral indices. *European Journal of Remote Sensing*. 54(1): 487-512. <https://doi.org/10.1080/22797254.2021.1965496>
- Guha, S., Govil, H. (2022). Annual assessment on the relationship between land surface temperature and six remote sensing indices using Landsat data from 1988 to 2019. *Geocarto International*. 37(15): 4292-4311. <https://doi.org/10.1080/10106049.2021.1886339>
- Guha, S., Govil, H., Taloor, A.K., Gill, N., Dey, A. (2022). Land surface temperature and spectral indices: A seasonal study of Raipur City. *Geodesy and Geodynamics*. 13(1): 72-82. <https://doi.org/10.1016/j.geog.2021.05.002>
- Kalota, D. (2017). Exploring relation of land surface temperature with selected variables using geographically weighted regression and ordinary least square methods in Manipur State, India. *Geocarto Int* 32(10): 1105-1119. <https://doi.org/10.1080/10106049.2016.1195883>
- Karakuş, C.B. (2019). The Impact of Land Use/Land Cover (LULC) Changes on Land Surface Temperature in Sivas City Center and Its Surroundings and Assessment of Urban Heat Island. *Asia-Pacific J Atmos Sci* 55: 669–684. <https://doi.org/10.1007/s13143-019-00109-w>
- Kundu, S., Khare, D., Mondal, A., Mishra, P.K. (2015). Analysis of spatial and temporal variation in rainfall trend of Madhya Pradesh, India (1901–2011). *Environ Earth Sci* 73: 8197-8216.
- Kundu, S., Mondal, A., Khare, D., Hain, C., Lakshmi, V. (2018). Projecting climate and land use change impacts on actual evapotranspiration for the Narmada River basin in central India in the future. *Remote Sens* 10(4): 578.
- Mondal, A., Guha, S., Kundu, S. (2021). Dynamic status of land surface temperature and spectral indices in Imphal city, India from 1991 to 2021. *Geomatics, Natural Hazards and Risk*. 12(1): 3265-3286. <https://doi.org/10.1080/19475705.2021.2008023>
- Mondal, A., Khare, D., Kundu, S. (2016a). Impact assessment of climate change on future soil erosion and SOC loss. *Nat Haz* 82: 1515-1539.
- Mondal, A., Khare, D., Kundu, S. (2016b). Change in rainfall erosivity in the past and future due to climate change in the central part of India. *Int Soil Water Conserv Res* 4 (3): 186–194.
- Mondal, A., Khare, D., Kundu, S. (2015). Spatial and temporal analysis of rainfall and temperature trend of India. *Theor appl climatol* 122: 143-158.
- Mondal, A., Lakshmi, V., Hashemi, H. (2018). Intercomparison of trend analysis of multisatellite monthly precipitation products and gauge measurements for river basins of India. *J Hydrol* 565: 779-790.
- Mushore, T.D., Mutanga, O., Odindi, J. (2022). Estimating urban LST using multiple

remotely sensed spectral indices and elevation retrievals, *Sustain Cities Soc* 78: 103623. <https://doi.org/10.1016/j.scs.2021.103623>

Pandey, A., Mondal, A., Guha, S., Upadhyay, P.K., Rashmi, (2022a). A Seasonal investigation on land surface temperature and spectral indices in Imphal city, India. *J Landsc Ecol* 15(3): 1-18. <https://doi.org/10.2478/jlecol-2022-0015>

Pandey, A., Mondal, A., Guha, S., Upadhyay, P.K., Rashmi, Kundu, S. (2023a). Analysis of Spectral Indices-Based Downscaled Land Surface Temperature in a humid subtropical city. *Int J Image Data Fusion*. <https://doi.org/10.1080/19479832.2023.2252818>

Pandey, A., Mondal, A., Guha, S., Upadhyay, P.K., Singh, D. (2022b). Land use status and its impact on land surface temperature in Imphal city, India. *Geol Ecol Landsc*. <http://dx.doi.org/10.1080/24749508.2022.2131962>

Pandey, A., Mondal, A., Guha, S., Upadhyay, P.K., Singh, D. (2023b). A long-term analysis of the dependency of land surface temperature on land surface indices. *Papers Appl Geog* 9(3): 279-294. <https://doi.org/10.1080/23754931.2023.2187314>

Peng, J., Xie, P., Liu, Y., Ma, J. (2016). Urban Thermal Environment Dynamics and Associated Landscape Pattern Factors: A Case Study in the Beijing Metropolitan Region. *Remote Sens Environ* 173: 145–155.

Sobrino, J.A., Raissouni, N., Li, Z. (2001). A comparative study of land surface emissivity retrieval from NOAA data. *Remote Sens Environ* 75(2): 256–266. [https://doi.org/10.1016/S0034-4257\(00\)00171-1](https://doi.org/10.1016/S0034-4257(00)00171-1)

Sobrino, J.A., Jimenez-Munoz, J.C., Paolini, L. (2004). Land surface temperature retrieval from Landsat TM5. *Remote Sens Environ* 9: 434–440. <https://doi:10.1016/j.rse.2004.02.003>

Tran, D.X., Pla, F., Latorre-Carmona, P., Myint, S.W., Caetano, M., Kieu, H.V. (2017). Characterizing the Relationship Between Land Use Land Cover Change and Land Surface Temperature. *ISPRS J Photogramm Sens* 124: 119–132.

Weng, Q.H., Lu, D.S., Schubring, J. (2004). Estimation of Land Surface Temperature–Vegetation Abundance Relationship for Urban Heat Island Studies. *Remote Sens Environ* 89: 467-483. <https://doi:10.1016/j.rse.2003.11.005>

Wiesner, S., Bechtel, B., Fischereit, J., Gruetzun, V., Hoffmann, P., Leidl, B., Rechid, D., Schlünzen, K.H., Thomsen, S. (2018). Is It Possible to Distinguish Global and Regional Climate Change from Urban Land Cover Induced Signals? A Mid-Latitude City Example. *Urban Sci* 2(1):12. <https://doi.org/10.3390/urbansci2010012>

Zhao, M., Cai, H., Qiao, Z., Xu, X. (2016). Influence of urban expansion on the urban heat island effect in Shanghai. *Int J Geogr Inf Sci* 30(12): 2421–2441. <https://doi.org/10.1080/13658816.2016.1178389>

Zhou, D., Xiao, J., Bonafoni, S., Berger, C., Deilami, K., Zhou, Y., Froelking, S., Yao, R., Qiao, Z., Sobrino, J.A. (2019). *Satellite Remote Sensing of Surface Urban Heat Islands: Progress, Challenges, and Perspectives*. *Remote Sens* 11: 48.

Web site:

-<https://www.ceicdata.com/en/india/census-population-by-towns-and-urban-agglomerations>

-<http://earthexplorer.usgs.gov/>

-<https://earth.google.com/web/>

-<https://imc.mn.gov.in/>

-<https://mausam.imd.gov.in/>